ADVANCED FUNCTIONAL MATERIALS
www.afm-journal.de

DNA/Tannic Acid Hybrid Gel Exhibiting Biodegradability, Extensibility, Tissue Adhesiveness, and Hemostatic Ability

*Mikyung Shin, Ji Hyun Ryu, Joseph P. Park, Keumyeon Kim, Jae Wook Yang, and Haeshin Lee**

DNA has emerged as a novel material in many areas of materials science due to its programmability. Especially, DNA hydrogels have been studied to incorporate new functions into gels. To date, only a few methods have been developed for fabricating DNA hydrogels, such as the use of complementary sequences or covalent bond. Herein, it is demonstrated that one of the most well-known plant-derived polyphenols, tannic acid (TA), can form a DNA hydrogel which is named TNA hydrogel (TA + DNA). TA plays a role as a "molecular glue" by a new mode of action reversibly connecting between phosphodiester bonds, which is different from the crosslinking utilizing complementary sequences. TA intrinsically degrades due to ester bonds connecting between pyrogallol groups, causing a degradable DNA hydrogel. Furthermore, TNA gel is multifunctional in that the gel is extensible upon pulling and adhesive to tissues because of the rich polyphenol groups in TA (ten phenols per TA). Unexpectedly, TNA gel exhibits superior in vivo hemostatic ability that can be useful for biomedical applications. This new DNA hydrogel preparation method represents a new technique for fabricating a large amount of DNA-based hemostatic hydrogel without chemically modifying DNA or requiring the crosslinking by complementary sequences.

1. Introduction

DNA is a remarkable candidate polymer for applications in materials science and biotechnology. Researchers have studied DNA for many purposes, such as for developing hydrogels,[1] DNA nanomachines,[2] and nanoscale DNA scaffolds,[3] carriers that can be used for drug delivery.[4] One important characteristic of DNA is its high molecular weight (≈3 million Da for typical 5 kb plasmids) compared with the molecular weights of other synthetic or natural polymers, for example, poly(ethylene glycol), alginate, hyaluronic acid, and dextran, which range from 10 to 100 kDa. Thus, DNA can be a good polymeric candidate for hydrogel formation; furthermore, DNA exhibits the unique properties of shape control and cell-free protein production.[1] The approaches to preparing DNA hydrogels have typically been based on complementary base-pairing, blending with cationic polymers, and covalent bond formation.[5] However, it would be desirable if a binder that is able to rapidly associate with and slowly dissociate from DNA molecules could be identified. Such an approach would not require any chemical modification of DNA for covalent-bond–driven hydrogel formation and might result in a large quantity of DNA hydrogel compared with that yielded by using complementary DNA.

Historically, hydrogels prepared by physical assembly have been extensively studied.[6] Most methods for preparing physically assembled hydrogels utilize interpolymeric chain interactions. Typically, the hydrophobic segment in a triblock copolymer, such as poly(propyl oxide) (PPO) or poly(D,L-lactide-co-glycolide) (PLGA), acts as a temperature-sensitive physical crosslinker.[7] Recently, a new concept called "molecular glue" in the field of physically assembled hydrogel fabrication has emerged. For example, the addition of dendrimers (the molecular glue) to clay nanosheets/sodium polyacrylate has been shown to result in mechanically strong yet moldable hydrogels.[8] Moreover, the addition of calcium ions (ionic glue) to alginate–polyacrylamide conjugates has provided highly stretchable and tough hydrogels.[9] Molecules such as cucurbit[*n*]uril[10] glue interpolymeric chains together to form hydrogels by well-known host–guest interactions.[11] As demonstrated in previous studies, the use of molecular glue is able to impart unique properties to hydrogels. However, the molecular glue concept has largely been limited to the formation of interpolymer chain linkages that do not provide additional functionalities such as tissue adhesion, degradation control, and extensibility. In addition, no study has focused on the use of the molecular glue concept for the preparation of DNA hydrogels.

M. Shin, Dr. J. H. Ryu, J. P. Park, Prof. H. Lee
The Graduate School of Nanoscience and Technology
Korea Advanced Institute of Science and Technology (KAIST)
291 University RdS
Daejeon 305-701, S. Korea
E-mail: haeshin@kaist.ac.kr
Dr. J. H. Ryu, Prof. H. Lee
Department of Chemistry
Korea Advanced Institute of Science and Technology (KAIST)
291 University Rd
Daejeon 305-701, S. Korea
K. Kim
R&D center, InnoTherapy
Daejeon 305-731, S. Korea
Prof.J. W. Yang
Department of Ophthalmology
Inje University Pusan Paik Hospital
Inje University College of Medicine
Busan 614-735, S. Korea

DOI: 10.1002/adfm.201403992

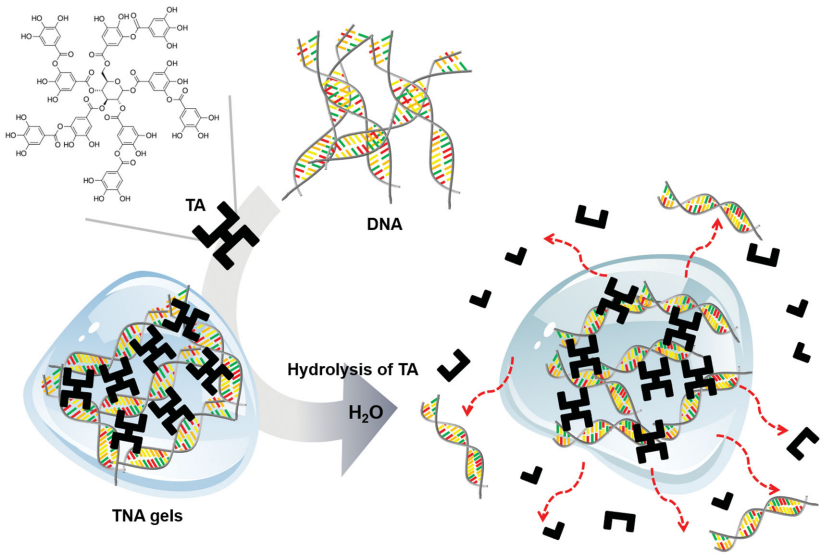

Figure 1. Schematic description of the formation and degradation of TNA gels.

In this study, we used tannic acid (TA), a molecule widely found in many plants,[12] as a molecular glue in the preparation of DNA hydrogels. TA is known for its reversible yet strong interactions with biomacromolecules, mostly proteins such as thrombin,[13] gelatin,[14] and elastin.[15] Especially, TA is the representative molecule responsible for developing unique astringency of wine and related beverage, which results from the interaction between TA and proline-rich proteins in saliva.[16] However, little is known about the interaction between TA and DNA. Thus, we hypothesized that TA can be a molecular glue for DNA hydrogel formation if there are significant inter-molecular interactions between the two. In fact, we observed that the simple addition of TA to DNA solution triggers the spontaneous formation of mechanically stable (>10 kPa) hydrogels, which are referred to as TNA (TA + DNA) gels. More recently, TA was used for multifunctional coating in material-independent surface chemistry, but the authors did not provide any insight into TA's interaction with DNA.[17] The chemical structure of TA shown in **Figure 1** indicates that the molecular glue is degradable and adhesive due to the presence of ester bonds and a number of catechol/pyrogallol groups (ten moieties per TA).[18] This structure can provide an advantage for the preparation of degradable, extensible, and adhesive DNA hydrogels. In addition, TNA gel has a novel hemostatic ability due to a number of phosphate groups in DNA backbone and the adhesiveness by TA acting as a tissue sealant, which might be suitable for biomedical applications.

2. Results and Discussion

Spontaneous TNA gelation was observed upon the addition of a TA solution (1 g mL^{-1} in distilled water, 40 µL, pH 1.6) to a DNA solution (5% in distilled water, 400 µL, pH 7.0–7.2). Under these conditions, the stoichiometric ratio of [DNA base pairs]/[TA] is 1.3 (**Figure 2**b, circle). When we changed the ratio [DNA base pairs]/[TA] to 2.6, no gelation occurred (Figure 2a). By contrast, when the ratio was further decreased from 1.3 to 0.9, mechanically robust TNA gels (3 → 30 kPa) were formed. It has been known that TA is oxidized above pH 7.[17] After the gelation, the pH value of TNA gel with [DNA base pairs]/[TA] ratio of 0.9 was about 4, and the value was increased to about 5 for the TNA gel with [DNA base pairs]/[TA] ratio of 1.3. Thus, we could anticipate that the oxidation of TA might largely be suppressed. It was difficult to prepare DNA solutions at concentrations greater than 5%. Additionally, TNA gels were not formed when the DNA concentration was lower than 2.5%. The elastic moduli (G′) were observed to increase in frequency sweeping experiments, indicating that TNA can forge intermolecular interactions via noncovalent, reversible bonds, such as hydrogen bonds. The increasing trend in the G′ value is characteristic for hydrogels composed entirely of noncovalent bonds. For example, catecholic hydrogels formed by metal coordination have shown similar increases in G′.[19] As expected, the incorporation of a large amount of TA (i.e., decrease in [DNA base pairs]/[TA] ratio) in hydrogel preparation resulted in mechanically stable hydrogels (circle to triangle, Figure 2b). Interestingly, TNA gels were formed when the stoichiometry of TA approached the number of DNA base pairs (i.e., [DNA base pairs]/[TA] = ≈1). The use of TA to prepare DNA gels is meaningful on a large scale (Figure 2c) at which TNA gels with an approximate volume of 113 000 mm^3 can be prepared easily. This volume is approximately 1000-fold higher than that of DNA hydrogels formed by using complementary base-pair binding.[1a] The advantages of DNA hydrogels constructed by complementary base-pair binding are innumerable, but the utility of these hydrogels is limited in applications that require a significant amount of DNA hydrogels that utilize simple functions of encapsulated DNA.

After lyophilizing TNA gels ([DNA base pair]/[TA] = 1.3), the cross-sectional morphology of the gels was investigated by scanning electron microscopy (SEM) (Figure S1, Supporting Information). The hydrogels exhibited a microporous structure similar to that of typical hydrogels.[20] In addition, the swelling ratio of TNA gels was measured: ≈6 for [DNA base pair]/[TA] of 0.9 and ≈13 for [DNA base pair]/[TA] of 1.3. This result is similar with the previously reported swelling ratio of calcium alginate fibrous gels.[21]

TA is composed of many hydrophilic polyphenols that consist of five catechols and five gallols at termini (Figure 1), which can interact with the phosphate backbone of DNA via hydrogen bonds. In fact, TA-mediated hydrogen bond formation was previously reported in which TA interacts with polyallylamine polymers via reversible hydrogen bonds or irreversible covalent crosslinking depending upon its pH conditions.[22] Thus, we hypothesized that the gel-to-sol transition might occur by breaking the hydrogen bonds upon heating. To verify our hypothesis, the temperature-dependent rheological

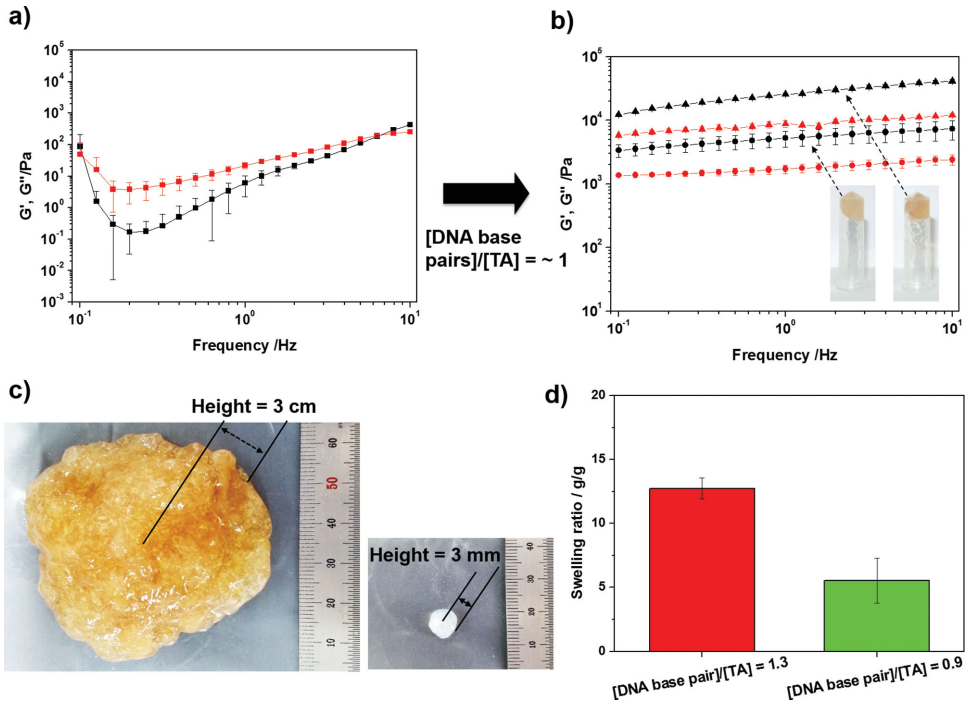

Figure 2. a,b) Mechanical properties of TNA gels (DNA concentration = 5%): frequency sweep experiments (elastic modulus (G′, black) and viscous modulus (G″, red)). The rheological properties of TA/DNA solutions as a function of stoichiometric ratio between the base pairs of DNA and TA. The [DNA base pairs]/[TA] ratios are 2.6 a), 1.3 b) (circle) and 0.9 b) (triangle). The inset photos show the gelation of the TA/DNA complexes ($n = 3$). c) A photo of TNA gels prepared on a large scale (left), which was compared with the typical volume of conventional, complementary base-pair crosslinked DNA hydrogel (right). d) The swelling ratio of the TNA gels. The TNA gel with [DNA base pair]/[TA] ratio of 0.9 (green). The gel with [DNA base pair]/[TA] ratio of 1.3 (red).

characteristics of TNA gels were measured from 30 to 70 °C (**Figure 3**). A previous Fourier-transform infrared spectroscopy (FT-IR) study demonstrated that hydrogen bond breakage occurs upon heating to 70 °C.[23] As expected, the temperature-dependent gel-to-sol transition was indeed observed at 54 °C for TNA gel with a [DNA base pair]/[TA] ratio of 1.3 (Figure 3a). The transition temperature did not change greatly even when the [DNA base pair]/[TA] ratio reached 0.9, demonstrating that the critical temperature was 55 °C (Figure 3b). This temperature-dependent change in physical properties indicates that the main mechanism involved in the formation of TNA gels is the creation of reversible hydrogen bonds.

To analyze the interaction between TA and DNA, a FT-IR study was performed by varying the [DNA base pair]/[TA] ratio (**Figure 4**a). In Figure 4a, the TA and DNA spectra are shown in blue and red, respectively, and spectra of the DNA/TA mixtures are shown in green, pink, and black. The wavenumber at which the antisymmetric vibration of phosphate groups initially appeared was 1238.22 cm^{-1} when the DNA was not mixed with TA;[24] this peak was largely shifted to 1199.64 cm^{-1} when the DNA was mixed with TA (red to black). Additionally, the ribose vibrational mode (C–C sugar) detected at 1095.49 cm^{-1}[24] was shifted to 1085.85 cm^{-1} (pink) when the DNA/TA mixture was prepared. In particular, when the stoichiometric ratio between the concentrations of TA and DNA base pairs was 1.3:1, which is the same stoichiometric condition used for typical TNA hydrogel preparation, we observed a split in the peak at 1095.49 cm^{-1} into two peaks at 1081.99 and 1033.77 cm^{-1} (black). This result indicates an enhanced interaction between TA and DNA. Furthermore, the overall shift in the peaks to lower wavenumbers suggests an increase in the DNA–TA interaction, particularly with OH–C (phenyl) from the gallol group of TA.[24] In addition, the deuteration of DNA can reveal the intermolecular interaction with other molecules, such as silica or cisplatin, via hydrogen bonds.[25] In D_2O, the phosphate vibrational frequency of DNA was downshifted from 1236.92 (Figure 4b, blue) to 1213.14 cm^{-1} (Figure 4b, red) upon addition of stoichiometric amounts of TA. This shift is larger than in H_2O, which is consistent with hydrogen bond interactions between TA and DNA that should show an isotope shift. Therefore, the driving force for the TA and DNA interactions is considered to be the formation of hydrogen bonds along the DNA phosphate backbone. The proposed overall interaction is schematically described in Figure 4c.

One of the unique characteristics of TNA gels is their degradability, which is derived from the hydrolyzable ester bonds connecting the catechol and pyrogallol groups in TA (TA structure, Figure 1). We hypothesized that the degradability of TA might result in the release of bound DNA molecules. This release could be an important phenomenon for biomedical applications. To explore the kinetic profile of DNA release from TNA gels, the gels were incubated in pH 7.4 Tris buffer (5 mL) at 37 °C, and sample solutions (100 µL for each) were collected at predetermined time intervals. To examine the amount of DNA released, we first tried to use an ultraviolet–visible (UV–vis) spectrophotometer. However, the quantification

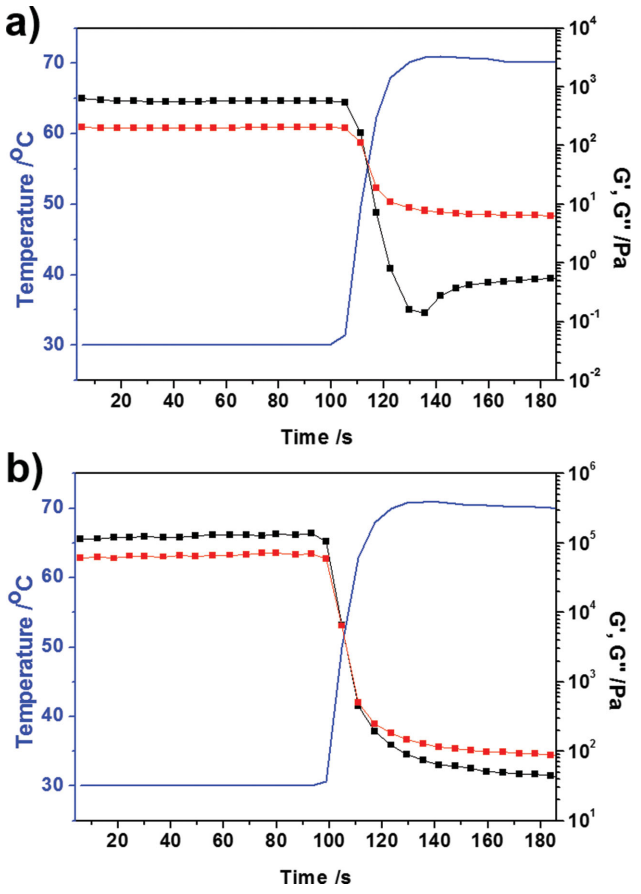

Figure 3. The gel-to-sol transition behavior of TNA gels. a) [DNA base pair]/[TA] = 1.3, and b) the ratio = 0.9. The blue trace indicates temperature changes. Elastic modulus (G′, black) and viscous modulus (G″, red).

of the DNA released was difficult because the molar extinction coefficient of DNA at 260 nm (ε_{260}, 6600 M^{-1} cm^{-1}) is much lower than that of TA at 250 nm (ε_{250}, 27 200 M^{-1} cm^{-1}) in UV absorption.[26] Therefore, the DNA release profile was analyzed indirectly by electrophoresis using 0.8% agarose gel. It should be noted that changes in DNA band intensity are generally used for quantification analysis in most studies. However, in our experiments, salmon sperm DNA was used, which is intrinsically polydisperse with respect to its molecular weight. Thus, an increase in DNA loading resulted in band broadening (i.e., an increase in vertical band height) (**Figure 5**a). As shown in lanes 2–8, the intensity and broadness of the DNA bands sampled from the supernatants of TNA gel solution gradually increased. For semiquantification, we loaded the same sperm DNA only: 4.2 μg for lane 9, 2.1 μg for lane 10, 1.0 μg for lane 11, and 0.5 μg for lane 12. From these DNA standard lanes, we could roughly estimate the amount of DNA released, which was 1.9 μg over a period of 24 h. The release profile of DNA from TNA gels was also analyzed by gel permeation chromatography (GPC) (Figure 5c). As time went by, the peak integration value of DNA released from TNA gel (11.6 min) increased from 3921.3 (black, 30 min) to 47 192.1 (dark cyan, 8 h). These data confirmed that the smeared bands appeared in the aforementioned gel electrophoresis were in fact DNA released from TNA gels. This DNA release is derived from the dissociation and degradation of the molecular glue, TA, which contains ester bonds connecting gallic acid and pyrogallol groups (Figure 1). To study the hydrolysis of TA and TA's dissociation from TNA gels, absorbance at 275 nm was measured for up to 96 h (Figure 5b). Owing to the large absorption overlap between TA (280 nm) and the hydrolyzed products of gallic acid (GA, 260 nm), ellagic acid (EA, 292 and 427 nm) and pyrogallol (PG, 267 nm), we chose 275 nm as the optimal wavelength for the three compounds (Figure S2, Supporting Information). As shown in Figure 5b, approximately 50% of the TA and the degradation products were released over 24 h; the amount of the compounds released then increased further and saturated at a level of 80% after 96 h. A previous high-performance liquid chromatography (HPLC) study demonstrated that the main degradation products of TA were GA, which was eluted for a retention time of 4.4 min, and EA, which was eluted for a retention time of 9.6 min (Figures S3 and S4a, Supporting Information).[18b] Additionally, the intensity of the weak PG peak corresponding to a retention time of 5.8 min gradually increased after 45 min. Actually, the peak integration value of these products increased from 3599 to 4401 for GA by the degradation of TA alone (Figure S4a, Supporting Information). Similarly, the value of EA increased from 2930 to 3986, and the value of PG increased from 0 to 366. For GA, the peak integration value of 4401 is equivalent to 0.1 μg, as determined by quantitative HPLC experiments (details are described in the Experimental Section). As shown in Figure S4b, Supporting Information, the peak integration value of heterogeneous TA with a retention time ranging from 11 to 30 min (Figure S3, Supporting Information) decreased, and the sum of the values for the degradation products gradually increased. Degradation and dissociation occurred in TNA gels were also investigated. As shown in Figure 5d, the peak of GA (6.0 min in Tris buffer, pH 7.4) increased dramatically within 1 h, and the peak of EA (14.7 min) increased after 3 h. In addition, the broad TA peak eluted after 17.6 min was subsequently appeared in a large amount after 3 h. Quantitative analysis exhibited the clear two-stage dissociation and degradation behavior of the TNA gels. At early time points (0.5 and 1 h), gallic acid and ellagic acid were predominantly found (the peak integration value of 957.4 for GA/EA degradation products and 525.5 for TA in 0.5 h; 6869.6 for GA/EA and 4447.1 for TA in 1 h) (Figure 5e, 1st and 2nd graphs). However, almost no dissociated TA was detected at the timeframes. At later time point (>3 h), TA was mainly dissociated from TA/DNA complexes followed by degradation of the dissociated TAs (220 946 for TA and 34 208 for GA/EA products in 3 h). These results indicate that TA/DNA complexes allow degradation of TA in low extent due to the steric hindrance of the complexed DNA at earlier time point. Subsequently, the dissociation of TA from TNA gels became a predominant phenomenon, which was detected at a later stage (>3 h). The dissociated TA can be a subject for rapid degradation resulting in increase of the amount of GA and EA products (Figure 5e, 3rd and 4th graphs). The schematic summary of the results was described in Figure 5f.

Other unexplored characteristics of TNA gel are its extensibility and tissue adhesion. To examine the extensibility and the adhesiveness of TNA gels, a universal testing machine (UTM) was used. For TNA gel extensibility experiments, TNA

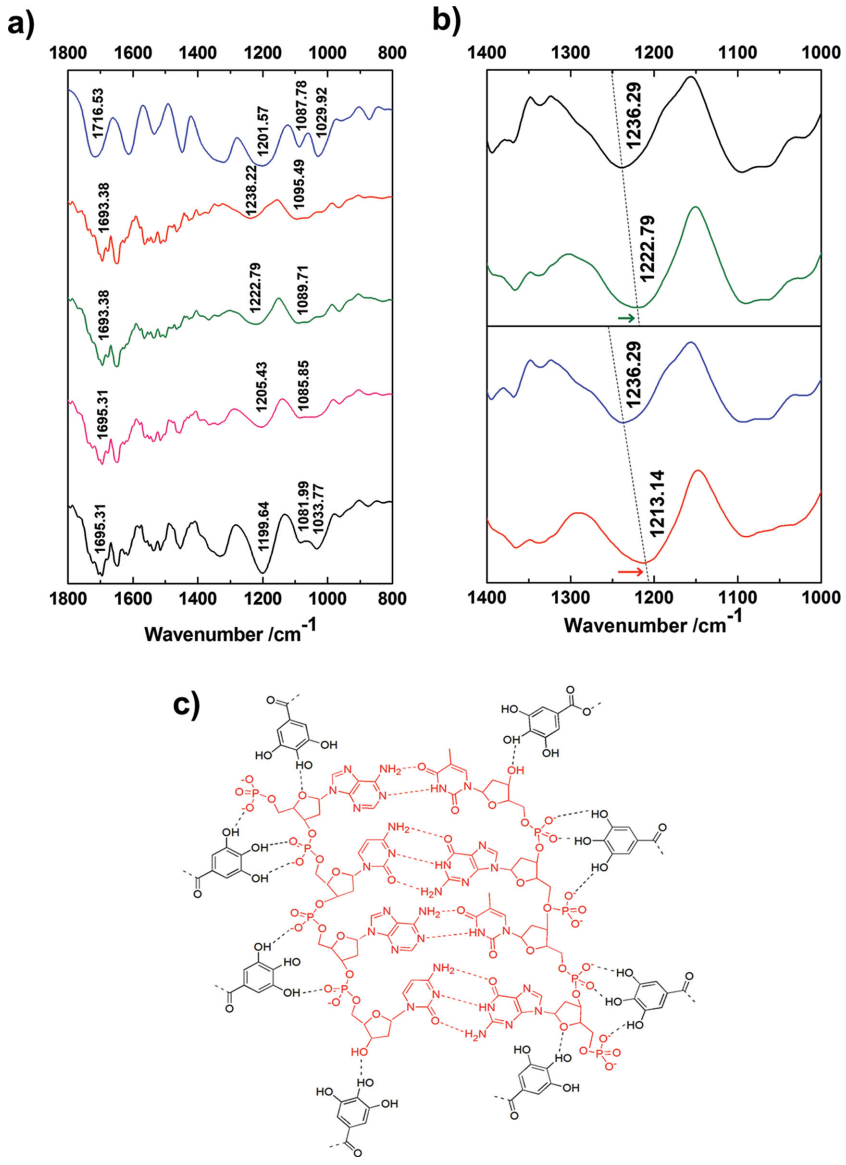

Figure 4. a) FT-IR spectra of DNA/TA mixture solutions in H_2O: TA alone (blue), DNA (red), TA/DNA mixture with the stoichiometric ratio of DNA base pairs: TA = 13.1:1 (green), the mixture with a ratio of 2.6:1 (pink) and the mixture with a ratio of 1.3:1 (black). b) The changes of the phosphate vibrational frequency by D_2O: DNA in H_2O (black), TA/DNA mixture with the stoichiometric ratio of DNA base pairs: TA = 13.1:1 in (green) in H_2O, DNA in D_2O (blue), and TA/DNA mixture with the same ratio (13.1:1) in D_2O (red). c) The proposed hydrogen bonding network (black dashed line) between DNA (red) and TA (black).

gel samples were prepared on overhead projector (OHP) films (**Figure 6**a, left), and the UTM force probes were then moved over the films at a speed of 1.5 cm min^{-1}. TNA gel with a [DNA base pairs]/[TA] ratio of 1.3 showed superior extensibility, up to 30 mm (Figure 6a, right, black), relative to that of the gel with a [DNA base pairs]/[TA] ratio of 0.9, which showed an extensibility of up to ≈15 mm (Figure 6a, right, red). Figure 6b shows a photograph of the extension test setup for TNA gels. We could not measure the extensibility of pure DNA hydrogel because the DNA solution itself did not undergo gelation. The extensibility of TNA gel may be derived from the extremely high molecular weight of the DNA template. We used approximately 20 kbp DNA for this experiment, which corresponds to a molecular weight of 13 200 000 Da. This molecular weight is truly unprecedented compared with any other polymers that have been used to prepare hydrogels. The rearrangement and/or reconfiguration of DNA structures can be amplified by the gluing action of DA between DNAs, which might result in the extensibility we observed.

We hypothesized that the increase in the TA content in TNA gels could enhance the adhesiveness of the gels. In Figure 6c, the adhesiveness of TNA gels increased compared with that of native DNA, 1.0 ± 1.0 kPa (black), reaching values of 10.5 ± 0.2 kPa for [DNA base pair]/[TA] = 1.3 (red) and 33.9 ± 2.1 kPa for [DNA base pair]/[TA] = 0.9 (green). The adhesiveness of the gel may be derived from TA because polyphenols have shown robust water-resistant adhesion in many biological systems, such as marine mussels and sandcastle worms.[27] In fact, TA alone showed significant adhesion: 75.4 kPa for 1 g mL^{-1} of TA and 98.1 kPa for 1.5 g mL^{-1} of TA (data not shown). Owing to their superior adhesion properties, TNA gels could tightly adhere to subcutaneous tissues (Figure 6d). TNA gels (≈150 mg) could bear the force of gravity sustained by ≈240 mg of the tissue. The results indicate that TNA gels have the potential for biomedical application as controllable adhesives and exhibit strong mechanical properties due to the stoichiometric ratio of TA to DNA base pairs. Strategies for introducing adhesion properties into biomacromolecules have mostly included the chemical tethering of catechol groups to various polymers, such as poly(ethylene glycol),[28] hyaluronic acid,[29] alginate,[30] chitosan,[31] dextran,[32] and others.[33] However, the introduction of adhesive properties into DNA has been a challenging task due to the difficulty of chemically modifying the backbone of the molecule. Considering the importance of DNA-related technologies, for example, drug delivery systems, the preparation of simple mixtures of TA and DNA can be a useful, practical method for formulating DNA hydrogels.

Finally, we demonstrated a new property of TNA gel that can potentially be useful for biomedical applications. We hypothesized that TNA gels might exhibit good hemostatic capability. In general, polyphosphate has been known as a hemostatic agent, which initiates blood clotting and activates fibrinolysis.[34] DNA is similarly rich in polyphosphate because of the backbone chemical structure; thus, a number of phosphate groups could contribute to in vivo hemostasis. We also hypothesized that the adhesive property of TNA gels shown in the previous experiments can enhance hemostasis due to

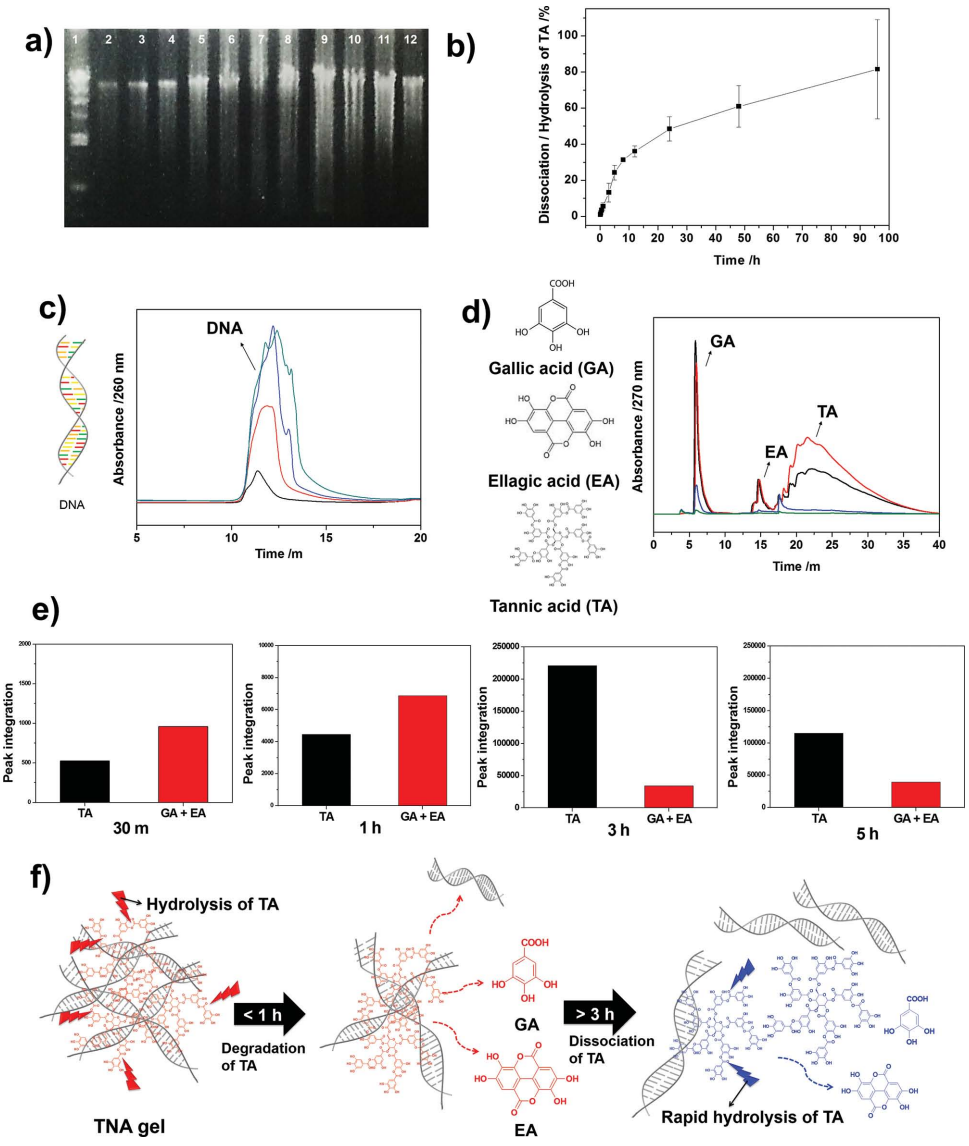

Figure 5. Results of the agarose electrophoresis experiment (0.8%) used to quantify the amount of DNA released from TNA gel. Lane 1 is the Lambda/Hind III marker. Lanes 2–8 are the DNA-released solution samples as a function of release time: 30 min (2), 1 h (3), 3 h (4), 5 h (5), 8 h (6), 12 h (7), and 24 h (8). Lanes 9–12 represent the predetermined amounts of salmon sperm DNA: 4.2, 2.1, 1.0, and 0.5 μg. The broadbands are due to the intrinsic polydispersity of salmon sperm DNA. b) Dissociation and hydrolysis kinetics of TA from TNA gels. c) Results of GPC studies for the DNA release profile from TNA gel (30 min for black, 1 h for red, 3 h for blue, and 8 h for dark cyan). d) Results of HPLC studies used to demonstrate the increases in hydrolyzed products of gallic acid (GA) and ellagic acid (EA) from TNA gel as a function of degradation time (30 min for green, 1 h for blue, 3 h for red, and 8 h for black). e) The HPLC peak integration results obtained in the panel c): the increase in GA and EA, the increase of TA dissociated from the gel after 1 h, and the decrease of TA by degradation after 3 h. f) The schematic summary for DNA release, the degradation and dissociation of TA.

sealing effect caused by tissue adhesion. For the hemostatic ability of TNA gels, a mouse liver bleeding model was used (**Figure 7**a, details are described in the Experimental Section).[35] First, as a negative control, the required time for complete hemostasis was measured without any treatment, which took 133 s (Figure 7b, black). Second, the single-component polymer solutions such as a solution dissolved in DNA only or a solution of TA only were used to study hemostatic effect, respectively, which was 97 s for DNA (Figure 7b, red) and 100 s for TA (Figure 7b, green). However, the time for hemostasis was greatly reduced down to about 53 s when using TNA gel (Figure 7b, blue). These results indicate that the hemostatic effect of TNA gel is a considerable level (133 → 53 s) demonstrating that TNA gel might be useful for biomedical hemostatic agents. Furthermore, as shown in Figure 2c, the mass production of TNA gel contributes to a scalability of hemostatic TNA gel for future industrial production.

3. Conclusion

In conclusion, we prepared multifunctional TNA hydrogels with unprecedented multifunctionality simultaneously exhibiting biodegradability, extensibility, tissue adhesiveness, and

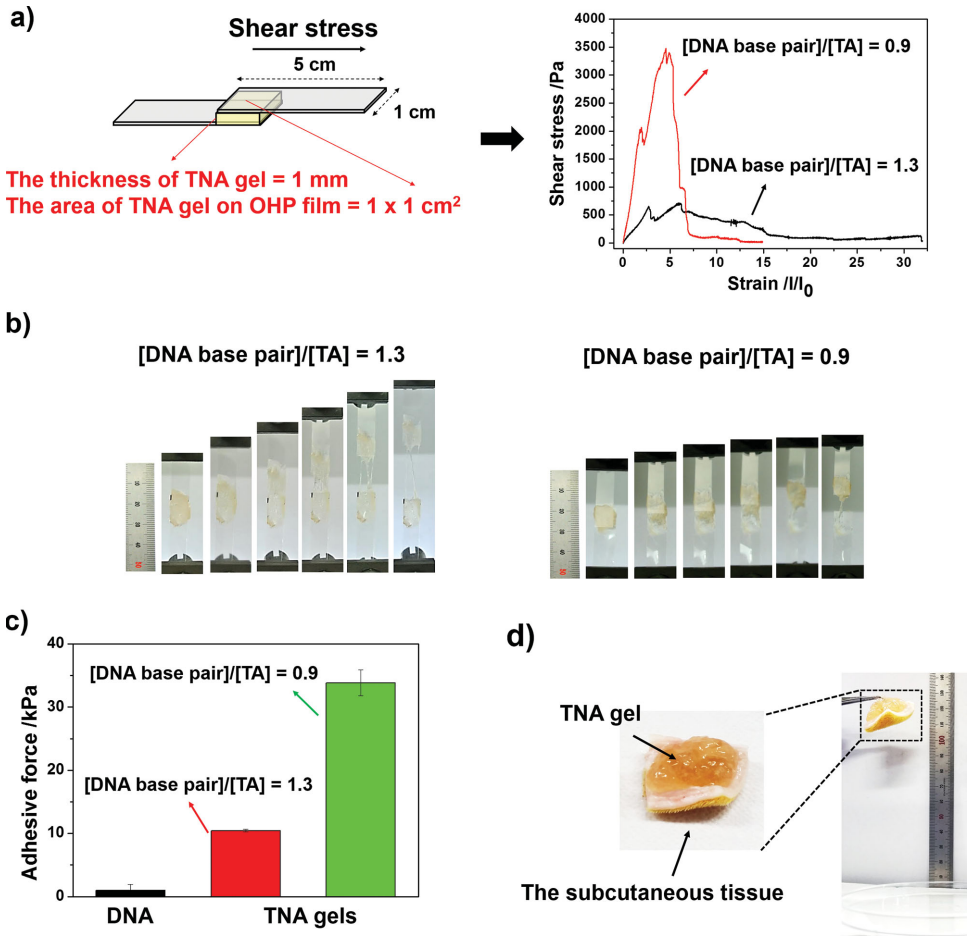

Figure 6. a) Shear stress–strain relationship of TNA gels. The experimental setup (left) and the force curves obtained from experiments (right): the gel with a stoichiometric ratio, [DNA base pair]/[TA], of 0.9 (red), and 1.3 (black). b) Series of photos captured to demonstrate the extensibility of TNA gels. c) The increase in adhesion force of TNA gels compared with that of DNA alone (black bar) and that in the presence of TA with a different stoichiometry (red and green). d) Results of the subcutaneous tissue adhesion test of TNA gel with a [DNA base pair]/[TA] ratio of 1.3.

hemostatic ability, using TA as a "molecular glue" without any chemical synthesis or by-products. TNA gels are multifunctional in the sense that the gels are extensible upon being pulled and adhesive toward biological tissues because of the large amount of polyphenol groups found in TA (ten phenols per TA molecule). Furthermore, the numerous ester groups of TA are hydrolyzed spontaneously upon exposure to physiological buffers, resulting in degradable TNA hydrogels. Because of its biodegradability, the encapsulated DNA was released from TNA gels, indicating that the gels can be useful systems for biomedical applications. In addition, we demonstrated for the first time that TNA gel could be a new platform as a DNA-based hemostatic agent. In contrast to the complementary base-pair binding utilized in the formation of conventional DNA hydrogels, TNA gel crosslinking mechanism forges hydrogel bonds between the phosphate backbone of DNA and the polyphenols of TA. Considering the facile preparation of large volumes of TNA gel afforded by the proposed method, our findings could be very useful for future biomedical applications that require adhesive, extensible, hemostatic gel agent with a great scalability.

4. Experimental Section

Materials: DNA from salmon testes and tannic acid (MW 1701.20) were purchased from Sigma-Aldrich (St. Louis, MO, USA). Gallic acid, pyrogallol, and ellagic acid were also obtained from Sigma-Aldrich.

Preparation of TNA Gels: DNA (approximately 20 000 base pairs) was dissolved in deionized water with a concentration of 5 w/v%, and TA was separately dissolved in deionized water with a concentration of 50, 100, or 150 w/v%. After 400 μL of the DNA solution was heated to 55 °C, 40 μL of the different concentrations (50, 100, or 150 w/v%) of TA solutions was added to the DNA solution. The hydrogels were incubated at room temperature for 30 min to complete the gelation induced by TA.

Rheological Studies and SEM Study of TNA Gels: The rheological properties of TNA gels were measured with a rotating rheometer equipped with a temperature controller (Bohlin Advanced Rheometer, Malvern Instruments, UK). TNA gels or TA/DNA sols (440 μL) were loaded on the 20 mm parallel plate. The test frequency was varied from 0.1 to 10 Hz, and all measurements were conducted under a constant stress of 100 Pa at room temperature. To test the gel-to-sol transition of TNA gels, the temperature was increased from 30 to 70 °C. Cross-sectional images of the lyophilized TNA gels were captured by SEM (Hitachi S-4800 FE-SEM, Japan).

Determination of the Swelling Ratio of TNA Gels: The gels were first dried at room temperature in vacuum oven for one day and were soaked

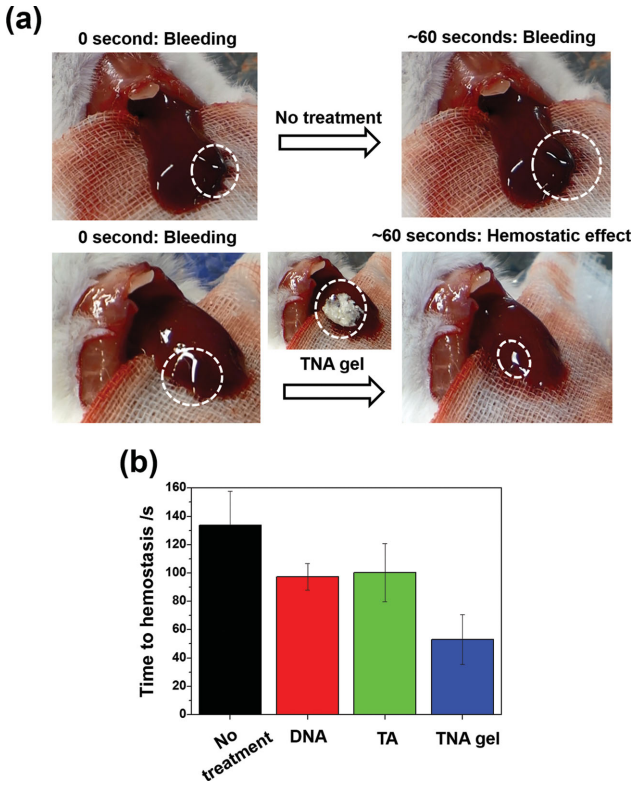

Figure 7. Hemostatic capability of TNA gels. a) The photo images for the hemostatic effect of TNA gels within 60 s: a control group without treatment (up), and sample groups treating TNA gel (bottom). b) The bar graph showing the required times for complete hemostasis in a bleeding mouse liver treated with DNA solution only (red), TA solution only (green), and TNA gel (blue).

in 5 mL Tris buffer (10×10^{-3} M, pH 7.4) at 37 °C. The weight of the swollen gels was measured after 15 min of hydration. The swelling ratio was calculated in the following equation

$$\text{Swelling ratio(g/g)} = \frac{(\text{The weight of the swollen gels} - \text{the weight of the dry gels})\text{(g)}}{\text{The weight of the dry gels(g)}}$$

FT-IR Study: To demonstrate the intermolecular interaction between DNA and TA, TA/DNA solutions with [DNA base pair]/[TA] ratios of 13.1, 2.6, and 1.3 were prepared. The molecular ratio was calculated by assuming that the average molecular weight of DNA base pairs was 660 g mol^{-1}. The lyophilized powders of TA, DNA, and the TA/DNA complex were dispersed in potassium bromide (KBr) and compressed into disks. The FT-IR spectra of the disks were obtained by performing 20 scans over the range of 400–4000 cm^{-1} using a Vector 33 spectrometer (Bruker, Germany).

In Vitro DNA Release: The Degradation and Dissociation of TA: TNA gels (246.8 mg) were placed on OHP films (1×1 cm^2) and incubated in 5 mL Tris buffer (pH 7.4) at 37 °C. After predetermined time intervals, the sample solutions (100 µL) were collected and then mixed with 100 µL fresh Tris buffer. To investigate the amounts of DNA released, 10 µL of the sample solution was loaded onto 0.8% agarose gel, and then electrophoresis was performed (Advance Co. Ltd., Tokyo, Japan). The amount of released DNA was analyzed by a Gel doc system (Bio-Rad, USA) and ImageJ software. In addition, to determine the degree of TA hydrolysis and dissociation, the absorbance (275 nm) of the sample solutions was measured by the diode array of an UV–vis spectrophotometer (HP8453, Hewlett Packard, USA). The tannic acid standard curves were established from 0.0056 to 0.0281 mg mL^{-1}. Furthermore, to demonstrate the release of DNA and the degradation of TA clearly, the sample solutions were analyzed by GPC for DNA and a reverse-phase liquid chromatography (RP-LC) (Agilent 1200, Santa Clara, CA, USA). In GPC study, Tris buffer (10×10^{-3} M, pH 7.4) was used as an eluent, and the UV–vis detector wavelength was set up to be 260 nm. In RP-LC study, the gradient of the mobile phase was as follows: 5% acetonitrile containing 0.1% trifluoroacetic acid (TFA) increased to 64% during the first 20 min and increased further to 95% for the next 10 min (i.e., 20–30 min), and subsequently decreased to 5% for the next 15 min (i.e., 30–45 min). The retention time was confirmed using an UV detector (270 nm). The flow rate for both chromatography was fixed to 0.5 mL min^{-1}.

The Short-Term Hydrolysis Profile of TA Using Reverse-Phase HPLC: The degradation products of TA were analyzed using a high-performance liquid chromatography system (Agilent 1200, Santa Clara, CA, USA). TA was dissolved in a pH 4 HCl solution (2 mg mL^{-1}) to inhibit the oxidation of pyrogallol groups. Gallic acid (0.5 mg mL^{-1}) was also dissolved in a pH 4 HCl solution, and ellagic acid (3 mg mL^{-1}) was dissolved in 1 M NaOH. The injection volume of model standard compounds (gallic acid, ellagic acid, pyrogallol, and TA) was 10 µL. Additionally, the solution that contained dissociated TA as well as degraded products from TA at a given time was also injected (10 µL). The gradient of the mobile phase was same with the Experimental Section for in vitro release test. The gallic acid standard curves for the peak integration were established as $y = 5078.9x + 843.2$ (where x = the amount of the gallic acid (µg) and y = the peak integration value).

UTM Study for the Extensibility and the Adhesive Force of TNA Gels and the Tissue Adhesion Test: To examine the extension and adhesion of TNA gels, a UTM test was conducted (Instron 5943, USA). The samples for the test were prepared using OHP films (1×5 cm^2). First, to test the extensibility of TNA gels, the gels were loaded between two films with a thickness of 1 mm (l_0) and an area of 1×1 cm^2. Shear stress was applied to the terminal of the gel-loaded films using a 50 N load cell at a rate of 15 mm min^{-1}, and the load (N) and the tensile extension (mm) were recorded by Instron Bluehill software. The final value for the stress–strain curve was calculated using the following equation

$$\text{Shear stress(Pa)} = \frac{\text{The load(N)}}{\text{The area}(m^2)}$$

$$\text{Strain(l/l0)} = \frac{\text{The tensile extension(mm)}}{\text{The initial thickness(mm)}}$$

Second, to test the adhesiveness of TNA gels, a small volume of the gels was compressed between OHP films with an area 1×1 cm^2. Similar to the extension test, shear stress was applied using a 500 N load cell at a rate of 10 mm min^{-1}. The adhesion force (kPa) was determined as the maximum load (kN) divided by the area (m^2). For the tissue adhesion test, the abdominal subcutaneous tissue (≈240 mg) of a rat (Sprague-Dawley rat, 8–9 weeks, male) was used. TNA gel (≈150 mg) was placed on the tissue and held there for almost 10 min to completely adhere to the tissue. When TNA gel was lifted, it was tested whether the gel could bear the tissue or not.

In Vivo Hemostatic Capability of TNA Gels: To examine in vivo hemostatic ability of TNA gels for biomedical application, a mouse (ICR mouse, eight weeks, male) hemorrhaging liver model was used.[35] Simply, a mouse was anesthetized using zoletil/rompun mixture. After abdominal incision, the medical gauze was placed beneath the mouse liver. The liver was washed using phosphate buffered saline (pH 7.4), and the bleeding was induced using a 23 G needle. As a negative control, the hemostatic time was measured without any treatment. After applying DNA solution (200 µL), TA solution (20 µL), and TNA gels (220 µL) on the bleeding site of the liver, the hemostatic time was also measured. All experiments were performed as triplicate. The animal experimental procedures and animal care were performed with the approval of the Animal Care Committee of KAIST (KA2014-34). In addition, The authors followed the ethical protocol given by the Korean Ministry of Health and Welfare.

Supporting Information

Supporting Information is available from the Wiley Online Library or from the author.

Acknowledgements

The authors are grateful for financial support from National Research Foundation of South Korea: Mid-career scientist grant (2014002855), molecular-level Interface Research Center (20090083525). Also, this study was supported in part by Korea Healthcare Technology R&D Project from the Ministry of Health and Welfare (HI12C0005).

Received: November 11, 2014
Revised: December 16, 2014
Published online: January 16, 2015

[1] a) S. H. Um, J. B. Lee, N. Park, S. Y. Kwon, C. C. Umbach, D. Luo, *Nat. Mater.* **2006**, *5*, 797; b) N. Park, S. H. Um, H. Funabashi, J. Xu, D. Luo, *Nat. Mater.* **2009**, *8*, 432.
[2] S. Surana, J. M. Bhat, S. P. Koushika, Y. Krishnan, *Nat. Commun.* **2011**, *2*, 1.
[3] N. C. Seeman, *Nature (London)* **2003**, *421*, 427.
[4] P. K. Lo, P. Karam, F. A. Aldaye, C. K. McLaughlin, G. D. Hamblin, G. Cosa, H. F. Sleiman, *Nat. Chem.* **2010**, *2*, 319.
[5] a) H. Tang, X. Duan, X. Feng, L. Liu, S. Wang, Y. Li, D. Zhu, *Chem. Commun.* **2009**, *6*, 641; b) D. Costa, J. Queiroz, M. G. Miguel, B. Lindman, *Colloids Surf. B* **2012**, *92*, 106; c) N. P. Truong, Z. Jia, M. Burgess, L. Payne, N. A. J. Mcmillan, M. J. Monteiro, *Biomacromolecules* **2011**, *12*, 3540.
[6] L. Yu, J. Ding, *Chem. Soc. Rev.* **2008**, *37*, 1473.
[7] a) B. Jeong, Y. K. Choia, Y. H. Baea, G. Zentnerb, S. W. Kim, *J. Controlled Release* **1999**, *62*, 109; b) C. He, S. W. Kim, D. S. Lee, *J. Controlled Release* **2008**, *127*, 189.
[8] Q. Wang, J. L. Mynar, M. Yoshida, E. Lee, M. Lee, K. Okuro, K. Kinbara, T. Aida, *Nature (London)* **2010**, *463*, 339.
[9] J. Sun, X. Zhao, W. R. K. Illeperuma, O. Chaudhuri, K. H. Oh, D. J. Mooney, J. J. Vlassak, Z. Suo, *Nature (London)* **2012**, *489*, 133.
[10] E. A. Appel, F. Biedermann, U. Rauwald, S. T. Jones, J. M. Zayed, O. A. Scherman, *J. Am. Chem. Soc.* **2010**, *132*, 14251.
[11] E. A. Appel, J. del Barrio, X. J. Loh, O. A. Scherman, *Chem. Soc. Rev.* **2012**, *41*, 6195.
[12] A. E. Hagerman, *J. Chem. Ecol.* **1987**, *13*, 437.
[13] A. Shukla, J. C. Fang, S. Puranam, F. R. Jensen, P. T. Hammond, *Adv. Mater.* **2012**, *24*, 492.
[14] J. P. Van Buren, W. B. Robinson, *J. Agric. Food Chem.* **1969**, *17*, 772.
[15] J. C. Isenburg, D. T. Simionescu, N. R. Vyavahare, *Biomaterials* **2004**, *25*, 3293.
[16] a) R. Gawel, *Austr.J. Grape Wine Res.* **1998**, *4*, 74; b) J. M. McRae, J. A. Kennedy, *Molecules* **2011**, *16*, 2348.
[17] a) T. S. Sileika, D. G. Barrett, R. Zhang, K. H. A. Lau, P. B. Messersmith, *Angew. Chem. Int. Ed.* **2013**, *52*, 10766; b) H. Ejima, J. J. Richardson, K. Liang, J. P. Best, M. P. Van Koeverden, G. K. Such, J. Cui, F. Caruso, *Science* **2013**, *341*, 154; c) J. Guo, Y. Ping, H. Ejima, K. Alt, M. Meissner, J. J. Richardson, Y. Yan, K. Peter, D. von Elverfeldt, C. E. Hagemeyer, F. Caruso, *Angew. Chem. Int. Ed.* **2014**, *53*, 5546.
[18] a) S. Quideau, D. Deffieux, C. Douat-Casassus, L. Pouysegu, *Angew. Chem. Int. Ed.* **2011**, *50*, 586; b) J. Zhu, J. Ng, L. J. Filippich, *J. Chromatogr.* **1992**, *577*, 77.
[19] a) D. G. Barrett, D. E. Fullenkamp, L. He, N. Holten-Andersen, K. Y. C. Lee, P. B. Messersmith, *Adv. Funct. Mater.* **2013**, *23*, 1111; b) N. Holten-Andersena, M. J. Harrington, H. Birkedal, B. P. Lee, P. B. Messersmith, K. Y. C. Lee, J. H. Waite, *Proc. Natl. Acad. Sci. USA* **2011**, *108*, 2651.
[20] J. Chen, K. Park, *J. Controlled Release* **2000**, *65*, 73.
[21] Y. Qin, *J. Appl. Polym. Sci.* **2004**, *91*, 1641.
[22] M. Krogsgaard, A. Andersen, H. Birkedal, *Chem. Commun.* **2014**, *50*, 13278.
[23] D. J. Skrovanek, S. E. Howe, P. C. Painter, M. M. Coleman, *Macromolecules* **1985**, *18*, 1676.
[24] a) S. Choosakoonkriang, C. M. Wiethoff, G. S. Koe, J. G. Koe, T. J. Anchordoquy, C. R. Middaugh, *J. Pharm. Sci.* **2003**, *92*, 115; b) M. M. Mady, W. A. Mohammed, N. M. El-Guendy, A. A. Elsayed, *Int. J. Phys. Sci.* **2011**, *6*, 7328.
[25] a) Y. Mao, L. N. Daniel, N. Whittaker, U. Saffiottil, *Environ. Health Perspect.* **1994**, *102*, 165; b) T. Theophanides, *Appl. Spectrosc.* **1981**, *35*, 461.
[26] a) L. C. Katwa, M. Ramakrishna, M. R. R. Rao, *J. Biosci.* **1981**, *3*, 135; b) K. W. Jennette, S. J. Lippard, G. A. Vassiliades, W. R. Bauer, *Proc. Natl. Acad. Sci. USA* **1974**, *71*, 3839.
[27] a) J. H. Waite, *Nat. Mater.* **2008**, *7*, 8; b) B. J. Endrizzi, R. J. Stewart, *J. Adhesion* **2009**, *85*, 546.
[28] a) J. L. Dalsin, B. Hu, B. P. Lee, P. B. Messersmith, *J. Am. Chem. Soc.* **2003**, *125*, 4353; b) X. Fan, L. Lin, J. L. Dalsin, P. B. Messersmith, *J. Am. Chem. Soc.* **2005**, *127*, 15843.
[29] a) S. Hong, K. Yang, B. Kang, C. Lee, I. T. Song, E. Byun, K. I. Park, S. Cho, H. Lee, *Adv. Funct. Mater.* **2013**, *23*, 1774; b) Y. Lee, H. Lee, Y. B. Kim, J. Kim, T. Hyeon, H. W. Park, P. B. Messersmith, T. G. Park, *Adv. Mater.* **2008**, *20*, 4154.
[30] a) C. J. Kastrup, M. Nahrendorf, J. L. Figueiredo, H. Lee, S. Kambhampat, T. Lee, S. Cho, R. Gorbatov, Y. Iwamoto, T. T. Dang, P. Dutta, J. H. Yeon, H. Cheng, C. D. Pritchard, A. J. Vegas, C. D. Siegel, S. MacDougall, M. Okonkwo, A. Thai, J. R. Stone, A. J. Coury, R. Weissleder, R. Langer, D. G. Anderson, *Proc. Natl. Acad. Sci. USA* **2012**, *109*, 21444; b) C. Lee, J. Shin, J. S. Lee, E. Byun, J. H. Ryu, S. H. Um, D. Kim, H. Lee, S. Cho, *Biomacromolecules* **2013**, *14*, 2004.
[31] a) K. Kim, J. H. Ryu, D. Y. Lee, H. Lee, *Biomater. Sci.* **2013**, *1*, 783; b) J. H. Ryu, Y. Lee, W. H. Kong, T. G. Kim, T. G. Park, H. Lee, *Biomacromolecules* **2011**, *12*, 2653.
[32] J. Y. Park, J. Yeom, J. S. Kim, M. Lee, H. Lee, Y. S. Nam, *Macromol. Biosci.* **2013**, *13*, 1511.
[33] E. Kim, I. T. Song, S. Lee, J. Kim, H. Lee, J. Jang, *Angew. Chem. Int. Ed.* **2012**, *51*, 5598.
[34] a) S. A. Smith, N. J. Mutch, D. Baskar, P. Rohloff, R. Docampo, J. H. Morrissey, *Proc. Natl. Acad. Sci. USA* **2006**, *103*, 903; b) J. H. Morrissey, S. H. Choi, S. A. Smith, *Blood* **2012**, *119*, 5972.
[35] Y. Murakami, M. Yokoyama, H. Nishida, Y. Tomizawa, H. Kurosawa, *J. Biomed. Mater. Res. B* **2009**, *91*, 102.